

Response times of meteorological air temperature sensors

Article

Published Version

Open Access

Burt, S. and de Podesta, M. (2020) Response times of meteorological air temperature sensors. *Quarterly Journal of the Royal Meteorological Society*, 146 (731). pp. 2789-2800. ISSN 1477-870X doi: <https://doi.org/10.1002/qj.3817> Available at <http://centaur.reading.ac.uk/90725/>

It is advisable to refer to the publisher's version if you intend to cite from the work. See [Guidance on citing](#).

Published version at: <https://doi.org/10.1002/qj.3817>

To link to this article DOI: <http://dx.doi.org/10.1002/qj.3817>

Publisher: Royal Meteorological Society

All outputs in CentAUR are protected by Intellectual Property Rights law, including copyright law. Copyright and IPR is retained by the creators or other copyright holders. Terms and conditions for use of this material are defined in the [End User Agreement](#).

www.reading.ac.uk/centaur

CentAUR

Central Archive at the University of Reading

Reading's research outputs online

RESEARCH ARTICLE

Response times of meteorological air temperature sensors

Stephen Burt¹  | Michael de Podesta² 

¹Department of Meteorology, University of Reading, Reading, UK

²National Physical Laboratory, Teddington, UK

Correspondence

Stephen Burt, Department of Meteorology, University of Reading, RG6 6BB, Reading, UK.

Email: s.d.burt@reading.ac.uk

Abstract

Guidelines in the *Guide to Meteorological Instruments and Methods of Observation* (the CIMO guide) of the World Meteorological Organization (WMO, published 2014, updated 2017, section 2.1.3.3, *Response times of thermometers*) recommend that the 63% response time τ for an air temperature sensor be 20 s, although – as airflow speed influences response time – the minimum airflow speed at which this applies should also be specified in the document. A 63% response time $\tau_{63} = 20$ s implies that 95% of a step change be registered within $3\tau_{63}$ or 60 s, the WMO recommended averaging interval for air temperature: rapid air temperature changes on this time-scale are not uncommon, often associated with convective squalls, frontal systems or sea breeze circulations. An alternative way of expressing the effect of the time constant is that in air whose temperature is changing at $0.1 \text{ K}\cdot\text{min}^{-1}$ the thermometer would lag by approximately 0.03 K.

To assess whether this response time specification was realistic, we have undertaken an experimental and theoretical study of the time constants of meteorological thermometers. Laboratory wind tunnel tests were undertaken to quantify 63% and 95% response times of 25 commercial 100Ω platinum resistance thermometers (PRTs) of various sizes (length and sheath diameter) from five manufacturers. The test results revealed a fourfold difference in response times between different sensors: none of the PRTs tested met the CIMO response time guideline at a ventilation speed of $1 \text{ m}\cdot\text{s}^{-1}$ assumed typical of passively ventilated thermometer shields such as Stevenson-type thermometer screens. A theoretical model of the sensors was devised which matched the experimental behaviour with regard to the most important contributing factors, namely ventilation rate and sensor diameter. Finally, suggestions and recommendations for operational air temperature sensor adoption and future sensor development are included.

KEYWORDS

air temperature, platinum resistance thermometer, response time, thermometer screen, WMO CIMO

1 | BACKGROUND AND MOTIVATION

1.1 | Meteorological relevance

Although the relative “sensitivity” of meteorological thermometry was first experimentally examined almost 150 years ago (Symons, 1875), it is perhaps surprising how little recent attention has been paid within the meteorological community to determining and optimising the response times of air temperature sensors. This is despite acknowledged recognition of the importance of sensor response time on meteorological temperature measurements, particularly maximum and minimum air temperatures, and the implications of differing sensor response times within a heterogeneous meteorological network are significant. A study by Lin and Hubbard (2008) noted instrumental biases in daily maximum and minimum air temperatures and diurnal temperature range resulting from variations in sampling rates, averaging algorithms and sensor time constants (implying degradation in between-site comparisons, whether in real-time or within long-term records), and recommended that such variations be reduced as far as possible to minimise resulting uncertainties in climatological datasets. More recently, Thorne *et al.* (2016) have included an extensive discussion of inhomogeneities in records of diurnal temperature range, noting that individual T_{MAX} and T_{MIN} data sets were more sensitive to inhomogeneities than their average. This observation highlights the significance of documenting changes in observational practice (including changes in sensor type or construction) when determining extreme temperatures.

Recent work by the Australian Bureau of Meteorology has quantified differing response times of “traditional” liquid-in-glass thermometry compared to faster-reacting electronic sensors (Benbow *et al.*, 2018) to assess possible lack of record consistency, particularly as “manual” observing sites transition to automatic weather station sensors (see also Box 1). Much of the (rather scant) literature on mercury-in-glass or PRT response times concerns industrial or biomedical temperature sensors, some of which require a much wider or much narrower range of operating temperatures than meteorological applications, lower precision and/or much less demanding requirements in terms of long-term calibration stability (years to decades): examples include Chohan and Hashemian (1989), Mackowiak and Worden (1994), Khorshid *et al.* (2005), Kyriacou (2010) and Niven *et al.* (2015).

Response times in stirred liquids (often water) are more frequently quoted than response times in gases: the relevant British Standards Institution Standard BS

EN 60751:2008¹ (British Standards Institution, 2008) specifies that PRT response times to 50% response should be measured in flowing water (at $0.2 \text{ m}\cdot\text{s}^{-1}$) and flowing air (at $3 \text{ m}\cdot\text{s}^{-1}$), although mandatory performance compliance levels are not set out. Incompletely considered changes in meteorological networks, particularly the wholesale substitution of sensors whose response rate or measuring/sample times differ significantly from historical methods of determination of air temperatures (usually liquid-in-glass thermometry) run the risk of introducing significant inhomogeneities into long-term temperature records: US examples have been given by Hubbard *et al.* (2001; 2004), and Doesken (2005). In Europe, Hannak *et al.* (2020) examined the variable impact of site automation using parallel daily mean temperature series. In addition, the bringing together of meteorology and metrology groups within Europe to work on areas of common importance within recent years has, and continues to bring, both clarity and benefits to meteorological metrology (Merlone *et al.*, 2015) and a forensic examination of environmental extremes (Merlone *et al.*, 2019).

Of course, the pursuit of shorter and shorter time constants to enhance sensor responsiveness in meteorological measurements of air temperatures is desirable only up to a point. Unlike wind speeds, for example, there is little benefit in sampling air temperature every second outside of specific research applications, such as turbulence or eddy-correlation measurements. Very fast-reacting sensors could result in higher fluctuations, increased thermal noise and relatively greater impacts from other environmental factors, such as rapid changes in wind speed or solar radiation. Rapid changes in external conditions in passively ventilated screens or radiation shields fitted with very “fast” sensors would most likely lead to slightly higher maximum and slightly lower minimum air temperatures than those recorded by conventional instruments in otherwise identical exposures, for no reason other than differences in instrumental responsiveness (see also Burt (2012), Chapter 5, *Measuring the temperature of the air*, for a longer discussion regarding operational perspectives). It is for this reason that WMO recommend (WMO, 2014, section 2.1.3.3 and Annex 1E) sampling air temperature every 5–10 s where feasible to do so, and averaging these samples to derive 60 s running means; and further that the highest and lowest (respectively) of the 60 s running average samples be logged as the day's maximum and minimum air temperatures. A consistent approach to sensor time constant and averaging time would improve consistency within and between station networks, as previously noted by Lin and Hubbard (2008), and would over time

¹This is identical to European Standard EN 60751 of the European Committee for Electrotechnical Standardization, CENELEC.

BOX 1 PRT response times compared to liquid-in-glass thermometers

In a similar recent laboratory study, Benbow *et al.* (2018) compared the response times for the three most commonly used Australian Bureau of Meteorology standard liquid-in-glass thermometers with a 4 mm diameter PRT as follows (data taken from their appendix A):

Sensor type	Samples	Average response time to 63%, with standard deviation: seconds	
		At 0 m s ⁻¹ airflow	At 3 m s ⁻¹ airflow
Thermometer, mercury-in-glass “ordinary” pattern	9	147 ± 9 s	55 ± 4 s
Thermometer, mercury-in-glass “maximum” pattern	9	211 ± 44	69 ± 10
Thermometer, alcohol-in-glass “minimum” pattern	10	277 ± 12	81 ± 3
PRT, 4 mm diameter	10	95 ± 17	35 ± 5

benefit the consistency of long-term climatological records of maximum and minimum temperatures and diurnal temperature range (Thorne *et al.*, 2016) – albeit at the risk of introducing some inhomogeneity at changeover unless both “old” and “new” records were maintained in parallel for an overlap period. To evaluate their suitability for meteorological air temperature records, measurements of the time constants of representative commercial sensors were determined by laboratory experiment and the results compared with a theoretical model.

1.2 | Response time theory

For a sensor with heat capacity C in thermal contact with air at temperature T_{air} through an effective thermal resistance R_{th} , the rate of change with time t of the thermometer temperature T is given by:

$$\frac{dT}{dt} = \frac{(T_{\text{air}} - T)}{R_{\text{th}}C}, \quad (1)$$

where $R_{\text{th}}C$ is known as the time constant, τ .

Following an instantaneous step change in the air temperature from T_0 to T_1 , a thermometer will respond to the change according to:

$$T(t) = T_0 + (T_1 - T_0)[1 - \exp[-t/\tau]]. \quad (2)$$

For $t \gg \tau$ the exponential term will diminish and the sensor's temperature T will approach T_1 . When $t = \tau$, the sensor will have registered 63% of the incremental change $(T_1 - T_0)$, while after 3τ , it will have registered 95% of the change. The time constant for a sensor response quoted by manufacturers may be quite different (e.g. time to reach 50% of a step change) and so for clarity we will henceforth refer to this exponential time constant as τ_{63} .

Step changes are unusual in meteorological air temperature measurements; instead the effect of the finite sensor time-constant is to cause the sensor to lag behind the actual air temperature by:

$$T(t) = T_{\text{air}}(t) - \tau_{63} \frac{dT_{\text{air}}}{dt}. \quad (3)$$

Thus for a sensor which meets the Commission for Instruments and Methods of Observation (CI MO) guideline of $\tau_{63}=20$ s, a change of air temperature at $0.1 \text{ K} \cdot \text{min}^{-1}$ would result in a temperature error of approximately 0.03 K; this would be considered acceptable in most meteorological applications (see Box 2). But for longer time constants and more rapid changes, errors could easily exceed 0.1 K. For a more detailed treatment, see Harrison (2014), section 2.2.

2 | EXPERIMENTAL METHOD

Twenty-five PRTs varying in diameter and length from five suppliers were tested. Three samples of each sensor (all rated to IEC60751 Class A specification) were investigated to assess the extent of manufacturing variability. Measurements were also made on a single 2 mm bead thermistor which was expected to have a very short time constant, although in its “bare” form such devices are insufficiently robust for routine operational use. Each PRT was a four-wire sensor (thereby compensating for varying lead lengths and thus resistance) contained within a steel sheath; in one unit the sheath had ventilation holes at its tip, in all others the sheath was continuous. The sheath provides mechanical and chemical protection to the temperature-sensitive element, usually a thin-film chip (platinum deposited on an alumina substrate) typically 2 mm square fixed within the

BOX 2 Observed rates of air temperature change

How frequently does the air temperature change by more than 0.1 K in 1 minute? There are few published accounts of the rate of change of air temperature over the short intervals considered here, and thus the 2019 records from Stratfield Mortimer Observatory, located 10 km southwest of Reading in southern England, were examined to assess this. The site is an open exposure typical of a midlatitude temperate climate. The observatory logs three closely co-located and carefully calibrated measurements of air temperature – made within a Stevenson screen, an automatic weather station (AWS) “multiplate” radiation shield and a permanently-aspirated shield – using identical PRT sensors. These are polled at 0.1 Hz and the average of the previous six 0.1 Hz values logged every minute, per WMO CIMO recommendations. In laboratory tests, the τ_{63} time constants of the 3×50 mm commercial PRT sensors in use averaged 26.4 s at $1 \text{ m}\cdot\text{s}^{-1}$ airflow (more typical of the passively ventilated sensors) and 16.0 s at $3 \text{ m}\cdot\text{s}^{-1}$ airflow (relevant to the aspirated sensor, and complying with WMO CIMO specification), averaged across 20 samples.

For each of the three screen types, the frequency of temperature changes of magnitude $|\Delta T|$ (K) from 1 minute to the next within given ranges over a period of 11 months during 2019 were as follows (>99.9% data availability):

Percentage of records within limits for air temperature change (ΔT , K) between consecutive 1 minute logged records: Stratfield Mortimer Observatory, Berkshire, January to November 2019

Magnitude of 1 minute temperature change $ \Delta T $	Exposure		
	Stevenson screen	AWS multiplate shield	Aspirated shield
$ \Delta T \leq \pm 0.1 \text{ K}$	87.9%	84.6%	65.8%
$0.1 \text{ K} < \Delta T \leq 0.25 \text{ K}$	10.3	13.0	23.6
$0.25 \text{ K} < \Delta T \leq 0.5 \text{ K}$	1.7	2.2	8.7
$ \Delta T > 0.5 \text{ K}$	0.1	0.1	1.9
Min. and max. ΔT , K	-1.53, +0.97	-1.45, +0.89	-1.81, +1.57
Total observations	492,162	492,170	492,101

Of course, the measurements from the Stevenson screen and AWS multiplate shield must be expected to be an underestimate of the truth, owing to a combination of response time, averaging time and screen lag factors. The results from the aspirated shield can be expected to be closer to the truth, owing to the shorter sensor response time at aspirated airflow speeds and the lack of screen lag. Although these results strongly suggest that air temperature changes from minute to minute are more likely within 0.1 K than outside it – at least at this single midlatitude reference site, and of course other sites/climates may differ – there are clear indications that rapid temperature changes occur considerably more frequently than conventional (i.e. screen-based, relatively slow τ_{63} sensors) meteorological records would suggest. Thus with a 20 s time constant, even the aspirated sensor may be in error by $\sim 0.16 \text{ K}$ around 1.9% of the time.

sheath by resin (thermal paste or other “potting compound”) – illustrated schematically in Figure 1. The measured response time will be the “lumped” response time of all the components.

Two PRTs at a time were connected to a Campbell Scientific CR1000 logger using a four-wire configuration and their resistances found, from which their temperature was derived, which was then logged at 2 Hz. Both PRTs were then fitted into dry close-fitting holes drilled within a 2 kg block of aluminium and warmed to 35–40 °C by placing

the aluminium block within a beaker of warm water, and allowed to attain a constant temperature.

Time response evaluations were conducted in the cooling phase using a small laboratory wind tunnel (Figure 2) in which the ventilation provided by an integral axial fan could be adjusted to provide steady airflow at speeds between 0.5 and $3.0 \text{ m}\cdot\text{s}^{-1}$. Ventilation speed was measured by a compact thermal anemometer (Testo model 425) located centrally within the wind tunnel, and was held constant for each test within $\pm 5\%$. The wind tunnel

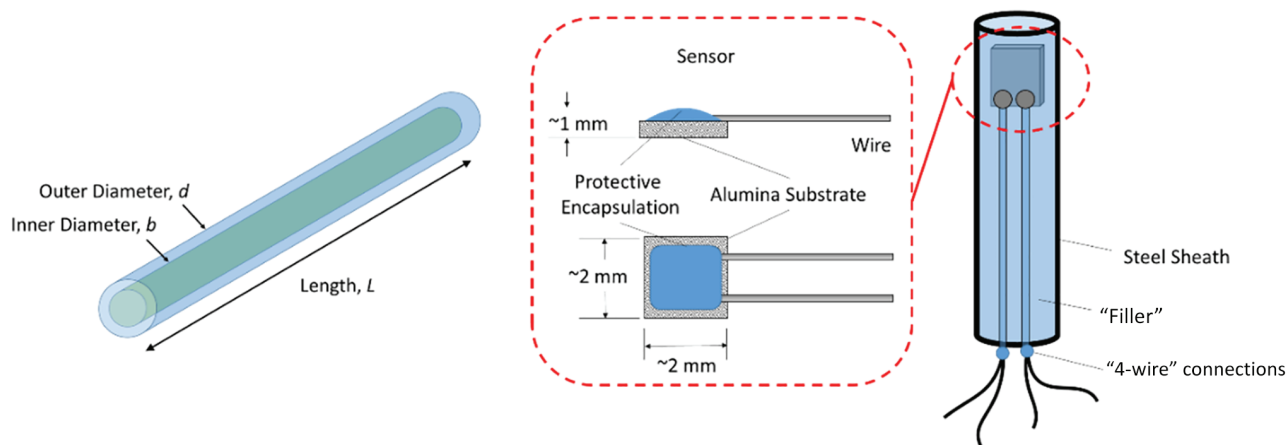


FIGURE 1 Schematic of typical commercial PRT. The internal diameter of the cylinder, b , is the external diameter d less twice the thickness of the steel sheath. Inset: Typical PRT sensor chip detail – based upon MN222 datasheet from Heraeus sensor technology GmbH, www.heraeus-sensor-technology.com

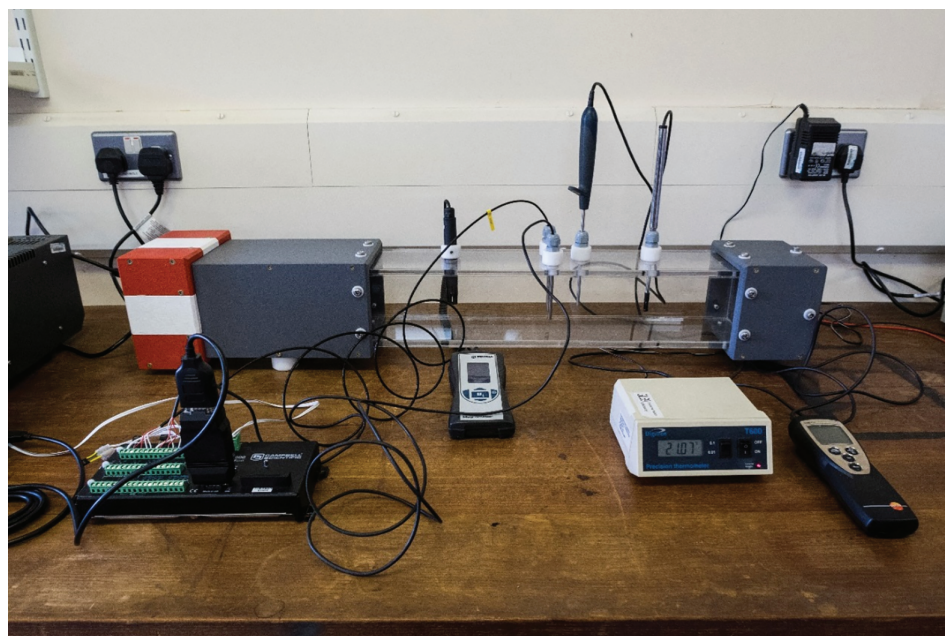


FIGURE 2 Experimental apparatus used to determine PRT response times: University of Reading, Department of Meteorology main laboratory. The desktop wind tunnel (Perspex) is shown nearest the wall; airflow is controlled by the fan at the left, and ventilation is from left to right. Sensors mounted within the tunnel airflow are (from left to right) a relative humidity (RH) sensor, the two PRTs under evaluation, a reference PRT and the compact thermal anemometer, all mounted within insulated fittings. The three displays on the desktop foreground are, left to right, RH, reference temperature and ventilation speed; the Campbell scientific CR1000 logger appears at left with PRTs connected. The logger is connected to a laptop computer displaying real-time graphical output of temperature from the two PRTs under test (not shown)

instrumentation also included a reference PRT (to monitor changes in ambient temperature) and a relative humidity (RH) sensor. No measurements were made of background irradiance levels, which are likely to have slightly affected the observed temperatures (de Podesta *et al.*, 2018); the occasional cycling of room heating within the laboratory was probably a greater source of error, although both are small in comparison with the 15–20 K cooling cycles used.

In this technique, the time constant deduced from the data is insensitive to key uncertainties affecting the inference of the temperature from the resistance measurement. In particular, the time constant is independent of any resistance offsets or linear calibration errors. Additionally, changes in the starting or finishing temperature are of little consequence as the time constant is derived from a fixed fraction of the temperature difference between the two,

once the rate of temperature fall has slowed to very close to zero.

After ensuring that the wind tunnel was at or very close to room temperature ($\sim 20^\circ\text{C}$), the airflow speed was adjusted to the desired level and allowed to settle for 1–2 minutes. At that point both PRTs were quickly removed from the aluminium block and inserted into the airflow of the wind tunnel, held in place by insulated mounting blocks. The temperature of each PRT was then logged until it fell close to the ambient laboratory temperature, after which it was returned to the aluminium block to warm up once more. This process was repeated for a minimum of four “runs” at each airflow velocity, initially at $0.5\text{ m}\cdot\text{s}^{-1}$ increments from 0.5 to $3.0\text{ m}\cdot\text{s}^{-1}$ (later streamlined to 0.5 , 1.0 and $3.0\text{ m}\cdot\text{s}^{-1}$, with intermediate results linearly interpolated) for each PRT. From the logged output, the time to reach 63% and 95% of the difference between the start temperature and steady-state room temperature was objectively evaluated for each sensor to within 0.25 s , and the mean and standard deviation from each set of runs calculated. In all, 502 individual evaluations were performed.

3 | MODELLING THE TIME CONSTANT

3.1 | Overview

The time constant τ_{63} depends on the product of the sensor heat capacity C and the thermal resistance between the sensor and the air R_{th} (Equation (1)).

If the sensor construction was homogenous, then we would expect the heat capacity to vary with the sensor volume that is, to vary with diameter and length as d^2L . However, the sensors have two main components: a stainless steel outer sheath, and an internal insulating filler. The heat capacity can thus be modelled as the sum of two components and the total heat capacity of the sensor C can be expressed as:

$$C = \pi(d^2 - b^2)L\rho_{\text{steel}}c_{\text{steel}} + \pi b^2L\rho_{\text{filler}}c_{\text{filler}}, \quad (4)$$

where ρ is the density and c is the specific heat capacity of the material.

In these experiments the specific heat capacity of the two components, and the relative amounts of each component in the sensor, are unknown but can be plausibly estimated. However, if the specific heat capacities of the two components are similar then we would still expect the heat capacity to scale roughly as $\sim d^2L$.

The thermal resistance between the sensor and the air is more difficult to estimate. A simple approach might

assume that the heat transfer was proportional to the exposed area of the cylinder πdL and the rate at which air which flowed past the sensor, v . However, as discussed in de Podesta *et al.* (2018), the air which flows past a cylinder forms a boundary layer that reduces the effectiveness of heat transfer per unit area for larger cylinders. The full expression for R_{th} taken from de Podesta *et al.* (2018) is:

$$R_{\text{th}} = \frac{d}{k \text{Nu}_{\text{cyl}}}, \quad (5)$$

$$\text{Nu}_{\text{cyl}} = 0.3 + \frac{0.62 \text{Re}^{1/2} \text{Pr}^{1/3}}{\left[1 + \left(\frac{0.4}{\text{Pr}}\right)^{2/3}\right]^{1/4}} \left[1 + \left(\frac{\text{Re}}{282000}\right)^{5/8}\right]^{4/5}, \quad (6)$$

where Re is the Reynolds number describing the flow and Pr is the Prandtl number describing the air. The Reynolds number is given by:

$$\text{Re} = \frac{\rho v d}{\mu}, \quad (7)$$

where ρ is the air density and μ is the air viscosity. The Prandtl number is given by:

$$\text{Pr} = \frac{v}{\alpha} = \frac{\mu c_p}{k}, \quad (8)$$

where α is the air thermal diffusivity and c_p is the specific heat capacity of the air. Equation (6) parametrizes an extremely complex process, but over a limited range of air speeds, the thermal resistance R_{th} is expected to vary as:

$$R_{\text{th}} \propto \frac{1}{L\sqrt{dv}}. \quad (9)$$

Combining our understanding of the way in which R_{th} and C scale with sensor size, we expect τ_{63} to vary roughly as:

$$\tau_{63} = R_{\text{th}}C \propto \frac{1}{L\sqrt{dv}} \times d^2L = \frac{d^{1.5}}{\sqrt{v}}. \quad (10)$$

From this result we expect τ_{63} to be independent of length, increase faster than linearly with diameter, and vary inversely as the square root of the air speed. A spreadsheet which encodes these formulae is downloadable from Figshare at <https://tinyurl.com/Burt-dePodesta-spreadsheet>.

3.2 | Model parameters

There are considerable uncertainties in the estimation of both R_{th} and C from first principles. Although there are no adjustable parameters in the estimation of R_{th} from

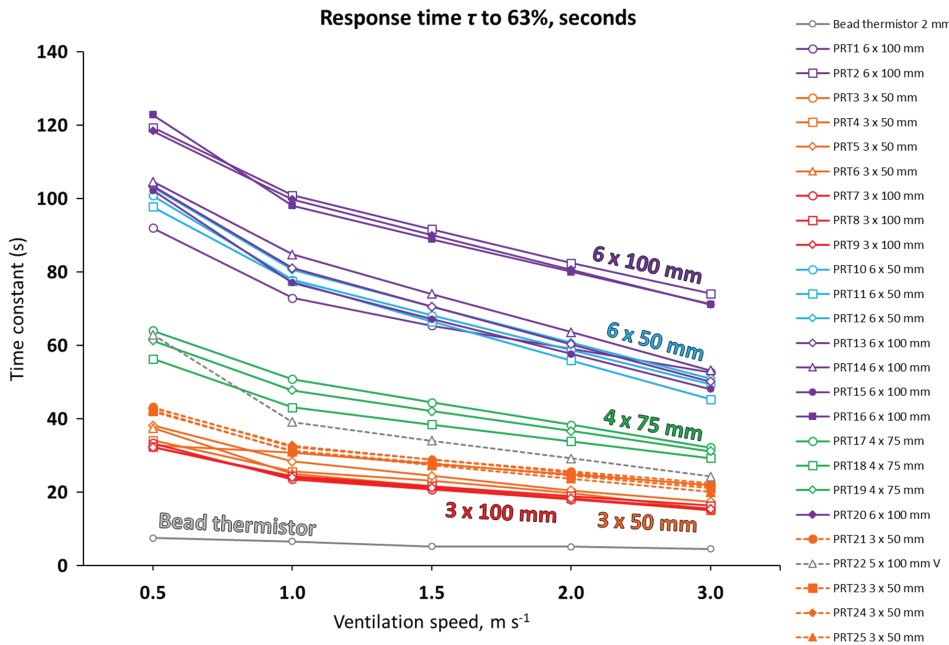


FIGURE 3 Individual response times (seconds) for the 2 mm bead thermistor and each of the 25 PRTs tested, plotted at each of the ventilation speeds from 0.5 to 3.0 m s⁻¹ (most of the 1.5 and 2.0 m s⁻¹ values are interpolations). Values are colour-coded by sensor size as shown in the legend on right. All sensors were sheathed; PRT22's sheath was ventilated (V) around the sensor tip

Equation (5), Çengel and Ghajar (2015) indicate that the uncertainty in Equation (9) is large – roughly 30%. The uncertainty in our estimation of the heat capacity of the sensors arises because we do not know their construction and composition.

We can estimate the overall heat capacity C by making reasonable assumptions about the sensor construction. We can make rough estimates by considering the sensor as a combination of an “inner cylinder” (containing the PRT chip, connecting leads and potting compound) and an “outer cylinder” (the exterior steel sheath) as illustrated in Figure 1. For a 6 mm diameter sensor 100 mm long, varying the thickness of the steel case from 0.5 to 1 mm, and varying the composition of the inner cylinder from alumina powder to epoxy resin, results in estimates of the sensor heat capacity which vary from 4 to 7.5 J·K⁻¹ that is, a variation of $\pm 30\%$ around the mean value. These results strongly suggest that differences in internal filling/potting compound formulation between manufacturers, and perhaps between individual sensors, exert a considerable influence on resulting sensor response times.

Given the large uncertainties in estimates of both R_{th} and C we should not expect our first-principles estimates of τ_{63} to be accurate to better than roughly $\pm 40\%$. However, we would expect τ_{63} to scale with sensor diameter d and length L in the manner expected from Equation (10).

4 | EXPERIMENTAL RESULTS AND DISCUSSION

Derived time constants by ventilation speed are shown for individual sensors in Figure 3, and results aggregated

by PRT form factor in Table 1. Manufacturers have been anonymised. For brevity, only the 63% response times τ_{63} are shown because 95% response times were, as expected, close to $3 \times \tau_{63}$ in all cases.

4.1 | Effect of ventilation

As expected (Harrison, 2014; de Podesta *et al.*, 2018) greater airflow speed resulted in increased advective heat transfer and consequently shorter response times. Of particular concern to the meteorological community was the result that the shortest individual τ_{63} at 1 m·s⁻¹ ventilation rate of all sensors tested was 23.6 ± 1.9 s (PRT7, 3 × 100 mm, average of five samples), still some way outside the WMO CIMO recommendation. Ventilation of 1 m s⁻¹ is the reference value assumed in ISO 17714, *Meteorology – Air temperature measurements – Test methods for comparing the performance of thermometer shields/screens and defining important characteristics* (ISO, 2007). Although there are as yet very few actual measurements of in-screen ventilation with which to compare, this air flow rate approximates to that believed to occur within a Stevenson-type radiation screen with an external wind speed of ≥ 2 m·s⁻¹.

Figure 4 shows experimental response times for various sensor diameters plotted versus the inverse square root of the ventilation speed. If the data are described by Equation 10, then we would expect the data to conform to a straight line through the origin, such as the fitted dotted lines. The fitted lines conform reasonably well to the data for the 3 and 5 mm diameter sensors, but do not describe the ventilation speed dependence of the larger

TABLE 1 PRT response times, grouped by sensor size and manufacturer

Sensor type, size and sample unit IDs	Mfr anonymised	No. of units	No. of samples		τ_{63} (s) for airflow v , $\text{m}\cdot\text{s}^{-1}$			
					0.5	1.0	2.0	3.0
Thermistor 2 mm bead	A	1	10	Mean	7.6	6.7	5.2	4.6
				SD	0.2	0.3	0.3	0.2
				Max	7.8	7.3	5.8	4.8
				Min	7.3	6.3	4.5	4.3
PRT 3 × 50 mm	B	1	5	Mean	32.8	30.9	24.9	22.0
				SD	1.3	0.6		0.5
				Max	34.3	31.5		22.3
				Min	31.0	29.8		21.0
PRT 3 × 50 mm	A	3	20	Mean	42.7	31.9	24.8	21.4
				SD	0.6	0.5		0.8
				Max	44.5	29.0		24.3
				Min	41.3	23.8		19.8
PRT 3 × 50 mm	C	3	20	Mean	36.7	26.4	19.6	16.0
				SD	1.7	1.0	1.1	0.5
				Max	40.5	29.0	22.5	22.3
				Min	28.8	23.8	18.5	14.5
PRT 3 × 100 mm	C	3	15	Mean	32.7	24.1	18.5	15.7
				SD	1.0	1.4		0.6
				Max	35.3	27.3		17.8
				Min	30.8	20.8		14.8
PRT 4 × 75 mm	D	3	15	Mean	60.6	47.3	36.3	30.9
				SD	1.8	1.2		1.5
				Max	66.8	52.8		34.3
				Min	54.5	41.8		26.8
PRT 5 × 100 mm	E	1	5	Mean	63.0	39.2	29.2	24.4
				SD	2.4	1.7		1.6
				Max	65.3	42.0		26.8
				Min	58.5	37.5		22.0
PRT 6 × 50 mm	C	3	15	Mean	100.6	78.7	58.5	48.6
				SD	1.9	1.6		1.5
				Max	107.3	81.8		53.3
				Min	94.3	75.3		43.0
PRT 6 × 100 mm	C	3	15	Mean	103.5	81.0	60.6	50.5
				SD	2.4	1.7		0.8
				Max	108.3	86.8		54.3
				Min	99.3	74.8		46.8
PRT 6 × 100 mm	B	4	25	Mean	113.2	93.0	75.6	67.4
				SD	2.4	2.7	2.1	1.8
				Max	125.8	107.3	85.0	77.3
				Min	88.3	70.3	53.0	50.8

Note: Average PRT response times (seconds) for 63% change τ_{63} by sensor size (sheath diameter $d \times$ length L , mm) and for different ventilation rates v , $\text{m}\cdot\text{s}^{-1}$, aggregated by sensor size and (anonymised) manufacturer. (Figure 3 shows results by individual PRT; this table shows sensor form factor averages). The sensor reference is per Figure 3, the number of sensors and number of samples for each ventilation rate are also shown. Results in *italic* are interpolated. Only the results shown in **bold** meet WMO CIMO specifications for meteorological air temperature sensors.

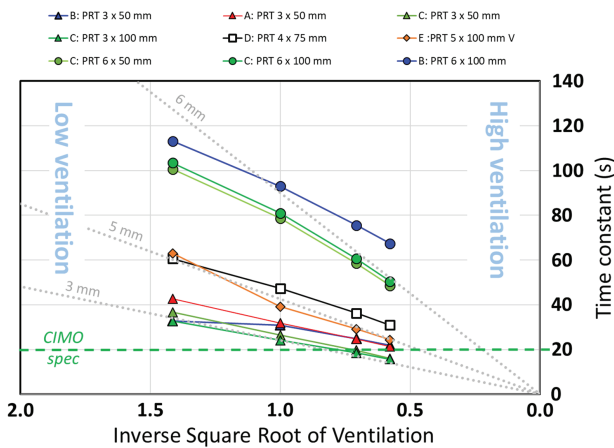


FIGURE 4 Mean sensor response times τ_{63} (s) from laboratory measurements (average by form factor and manufacturer) plotted versus the inverse square root of the ventilation speed $1/\sqrt{v}$. Manufacturers are indicated by letters A to E and by colour, sensor diameter shown by plotted shape (6 mm diameter as a circle, 5 mm diamond, 4 mm square, 3 mm triangle). If the data conform to the expected behaviour (Equation (10)), they should fall on straight lines through the origin shown by pale grey dotted lines for 3, 5 and 6 mm sensors. The CIMO response time τ_{63} guideline 20 s is shown by the dashed green line

diameter sensors. The reason for this behaviour is not understood.

The slowest individual sensor response time at $1 \text{ m}\cdot\text{s}^{-1}$ was $100.9 \pm 2.8 \text{ s}$ (PRT2, $6 \times 100 \text{ mm}$, four samples), more than five times the CIMO recommended specification. Average τ_{63} for this particular PRT (PRT2) ranged from 119.5 s at $0.5 \text{ m}\cdot\text{s}^{-1}$ to 74.2 s at $3 \text{ m}\cdot\text{s}^{-1}$. The measured τ_{95} at $0.5 \text{ m}\cdot\text{s}^{-1}$ for this sensor of $292 \text{ s} \pm 14 \text{ s}$ (average of five samples) implies that this particular device would be incapable of registering 95% of a step change in air temperature in under 5 minutes in light wind conditions. Alternatively, if the temperature was changing at 0.1 K per minute, the sensor would be in error by approximately 0.2 K. Clearly such a sensor would be better suited to applications where speed of response is secondary to sensor protection, for example in measurement of soil temperatures.

At $2 \text{ m}\cdot\text{s}^{-1}$ ventilation, only 20% of the samples (all small sensor diameter), were able to meet the WMO CIMO τ_{63} 20 s response time specification. Increasing ventilation to $3 \text{ m}\cdot\text{s}^{-1}$ did not increase this ratio, although one additional sensor lay just outside the specification. A $3 \text{ m}\cdot\text{s}^{-1}$ airflow is more typical of the minimum ventilation rate in permanently aspirated systems. This low level of compliance with WMO CIMO guideline specifications clearly implies that the majority of the commercial sensors tested would be unsuitable for air temperature measurements in either Stevenson-type thermometer screens or aspirated systems if compliance with WMO CIMO requirements were to become mandatory.

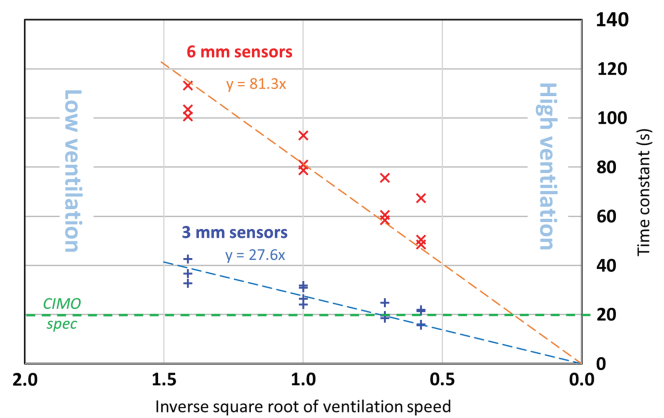


FIGURE 5 This shows the same data as in Figure 4 but re-plotted to include only 3 and 6 mm diameter sensors which have been lumped together as two datasets grouped by sensor diameter

4.2 | Effect of sensor size

Figure 5 shows the data from Figure 4 re-plotted to include only the 3 and 6 mm sensors now grouped together by diameter. The τ_{63} values for the sensors in the test are clearly grouped by diameter, rather than length or manufacturer. The ratio of the fitted slopes of the ventilation speed dependence is $81.3/27.6 = 2.94$. This can be compared with the expected difference based on the doubling of the sensor diameter of $2^{1.5} = 2.83$.

Informal discussions with suppliers suggested that the deviations from the trend are probably due to differences in the composition between the smaller- and larger-diameter thermometers. A typical sensor chip is only about 2 mm square, fitting snugly within a 3 mm sheath but insulated by a greater thickness of resin within a larger-diameter sheath (Figure 1).

4.3 | Rule of thumb

Analysing the data at a ventilation speed of $1 \text{ m}\cdot\text{s}^{-1}$ only, it was found that within a standard deviation of approximately 10%, the time constant of all the non-ventilated cylindrical sensors could be approximated as $\tau_{63} \approx 5.6 d^{3/2}$ seconds, where d is expressed in millimetres. The time constant is expected to scale inversely as the square root of the ventilation speed so as a rule-of-thumb, the time constant in seconds for conventionally constructed PRT sensors can be therefore estimated as:

$$\tau_{63} \approx 5.6 \frac{d^{3/2}}{v^{1/2}}, \tag{11}$$

where d is expressed in millimetres and v is expressed in metres per second. The data are re-plotted in this

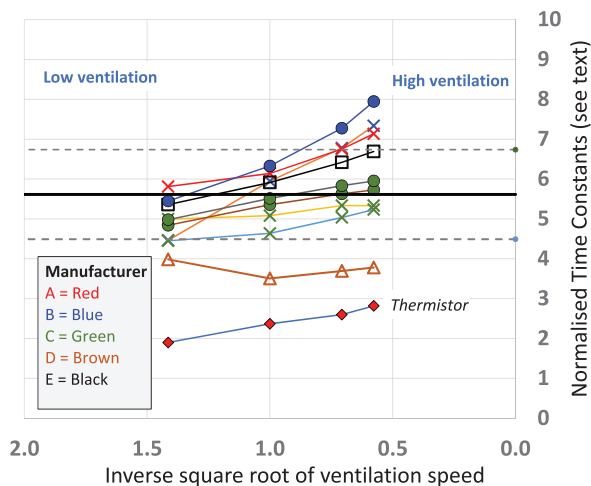


FIGURE 6 Comparison of experimental data with rule-of-thumb in Equation (11). The measured values of τ_{63} have been divided by $d^{3/2}$ and plotted versus $1/\sqrt{v}$. The data lie roughly within $\pm 20\%$ of the rule of thumb value

way in Figure 6. The rule-of-thumb describes most of the data within roughly $\pm 20\%$, but it is clear that it has not quite described the wind-speed dependence. The data indicate that at higher ventilation speeds the time constants are longer than would be expected based on the low-ventilation speed values of τ_{63} .

5 | SUMMARY AND CONCLUSIONS

This series of laboratory tests showed large variations in response times of commercial PRTs used for meteorological air temperature measurements. Numerical models of a cylinder cooled in horizontal airflow at various ventilation rates provided reasonable approximations to the experimental results and permitted examination of some of the variables affecting sensor performance.

The two most important factors were found to be ventilation rate and sensor diameter, the combination accounting for more than an order of magnitude difference in τ_{63} . It was particularly surprising to find that *none* of the PRTs tested met the WMO CIMO τ_{63} 20 s response time specification at a ventilation speed of $1 \text{ m}\cdot\text{s}^{-1}$ assumed typical of passively ventilated thermometer shields such as Stevenson-type thermometer screens, where sensor airflow depends nonlinearly upon ambient wind speed. It was found by experiment, and confirmed by modelling, that sub-20 s τ_{63} response times were attainable only with small diameter ($\leq 3 \text{ mm}$) PRT probes ventilated at $> 2 \text{ m}\cdot\text{s}^{-1}$, an airflow rate more typical of permanently aspirated systems. To attain sub-20 s τ_{63} response times at a ventilation speed of $1 \text{ m}\cdot\text{s}^{-1}$ would require sensors with diameter less

than 3 mm. Although smaller PRTs are available, many commercially available PRTs use a sensor chip which is itself a little over 2 mm in diameter (Figure 1), enclosed in a 0.5 mm thick steel sheath necessary to provide operational robustness and to protect the sensor chip from moisture, dust and atmospheric pollution.

Based upon these findings, the following recommendations are suggested:

1. For meteorological air temperature measurements, in order to meet WMO CIMO guidelines, PRTs no larger than 3 mm diameter should be specified in procurement tenders, particularly where the intended use is within passively ventilated thermometer screens (Stevenson-type or similar, or AWS “multi-plate” radiation shelters). Sensor length is less critical, but should be as short as operationally convenient to minimise sensor mass and unit costs: 25–50 mm for example.
2. Manufacturers and component suppliers should be expected to measure and specify both sensor diameter and τ_{63} response times at $1 \text{ m}\cdot\text{s}^{-1}$ ventilation in air in product specifications and in tender documents for all PRTs intended for meteorological air temperature measurements.
3. Manufacturers should be encouraged to optimise existing PRT design and assembly processes with a view to meeting or exceeding WMO CIMO sub-20 s τ_{63} PRT response time at a ventilation rate of $1 \text{ m}\cdot\text{s}^{-1}$ where this can be achieved without detriment to sensor robustness, calibration stability and conformity to IEC60751. Helpful changes could include changes to sensor placement within the sheath (as near the tip of the sheath as possible), optimising thermal contact between sensor and sheath (and hence with the external environment), and reducing the heat capacity of the potting compound as far as possible. Additionally, polishing or silvering the exterior surface of the sensor will reduce the sensitivity to radiation.
4. Provided they can be mass-produced at similar costs and levels of operational robustness for periods of use lasting a decade or more, smaller PRTs (1–2 mm diameter) should be developed and trialled for future meteorological air temperature measurements. The day-to-day handling requirements for such sensors, once installed, should be negligible, in contrast to fragile conventional liquid-in-glass thermometry.
5. The purpose of the WMO CIMO guide is to ensure that measurements made around the world are ultimately comparable with low uncertainty. We thus recommend updated guidance on response times and sensor selection be included in future revisions of the WMO CIMO guide.

ACKNOWLEDGEMENTS

The authors are most grateful to Giles Harrison (Department of Meteorology, University of Reading) for his support and inspiration. We are pleased to acknowledge the help of the several manufacturers – who unfortunately must remain anonymous – who provided commercial samples for evaluation in this experiment. We are grateful to Jane Warne (Australian Bureau of Meteorology) for helpful comments on an early draft of this article, and to Paul Copping (Fairmount Weather Systems) who provided material support to undertake the tests (Fairmount does not manufacture PRTs). We also offer thanks to the laboratory technical staff in the Department of Meteorology at the University of Reading, Andrew Lomas, Selena Zito and Ian Read in particular.

A preliminary version of the findings of this experiment was presented at the WMO Technical Conference on meteorological and environmental instruments and methods of observation (CIMO TECO-2018) in Amsterdam, the Netherlands, 8–11 October 2018.

ORCID

Stephen Burt  <https://orcid.org/0000-0002-5125-6546>

Michael de Podesta  <https://orcid.org/0000-0002-6635-6806>

REFERENCES

- Benbow, D., Dollery, I. and Warne, J. (2018) *Instrument Test Report 714: Response times of surface thermometers*. Australia: Bureau of Meteorology.
- British Standards Institution (2008) BS EN 60751:2008 – Industrial platinum resistance thermometers and platinum temperature sensors.
- Burt, S. (2012) *The Weather Observer's Handbook*. New York, NY: Cambridge University Press.
- Çengel, Y.A. and Ghajar, A.J. (2015) *Heat and Mass Transfer: Fundamentals and Application*. New York, NY: McGraw-Hill.
- Chohan, R.K. and Hashemian, M. (1989) Response time of platinum resistance thermometers in flowing gases. *Fire and Materials*, 14, 31–36.
- de Podesta, M., Bell, S. and Underwood, R. (2018) Air temperature sensors: dependence of radiative errors on sensor diameter in precision metrology and meteorology. *Metrologia*, 55, 229–244.
- Doesken, N.J. (2005) *The National Weather Service MMTS (Maximum–Minimum Temperature System) – 20 years after*. American Meteorological Society Conference Papers. <http://ams.confex.com/ams/pdfpapers/91613.pdf> Accessed 8 October 2019.
- Hannak, L., Friedrich, K., Imbery, F. and Kaspar, F. (2020) Analyzing the impact of automatization using parallel daily mean temperature series including breakpoint detection and homogenization. *International Journal of Climatology*. <https://doi.org/10.1002/joc.6597>.
- Harrison, R.G. (2014) *Meteorological Measurements and Instrumentation*. Chichester, UK: Wiley.
- Hubbard, K.G., Lin, X.M., Baker, C.B. and Sun, B. (2004) Air temperature comparison between the MMTS and the USCRN temperature systems. *Journal of Atmospheric and Oceanic Technology*, 21, 1590–1597.
- Hubbard, K.G., Lin, X.M. and Walter-Shea, E.A. (2001) The effectiveness of the ASOS, MMTS, Gill, and CRS air temperature radiation shields. *Journal of Atmospheric and Oceanic Technology*, 18, 851–864.
- International Organization for Standardization (ISO). (2007) *ISO 17714 meteorology – air temperature measurements – test methods for comparing the performance of thermometer shields/screens and defining important characteristics*. International Organization for Standardization (ISO); Geneva.
- Khorshid, L., Eşer, İ., Zaybak, A. and Yapucu, Ü. (2005) Comparing mercury-in-glass, tympanic and disposable thermometers in measuring body temperature in healthy young people. *Journal of Clinical Nursing*, 14, 496–500.
- Kyriacou, P.A. (2010) Biomedical sensors: temperature sensor technology. *Sensors Technology Series: Biomedical Sensors*, Chapter 1. New York, NY: Momentum Press
- Lin, X. and Hubbard, K.G. (2008) What are daily maximum and minimum temperatures in observed climatology? *International Journal of Climatology*, 28, 283–294.
- Mackowiak, P.A. and Worden, G. (1994) Carl Reinhold August Wunderlich and the evolution of clinical thermometry. *Clinical Infectious Diseases*, 18, 458–467.
- Merlone, A., Al-Dashti, H., Faisal, N., Cerveny, R.S., AlSarmi, S., Bessemoulin, P., Brunet, M., Driouech, F., Khalatyan, Y., Peterson, T.C., Rahimzadeh, F., Trewin, B., Wahab, M.M.A., Yagan, S., Coppa, G., Smorgon, D., Musacchio, C. and Krahenbuhl, D. (2019) Temperature extreme records: World Meteorological Organization metrological and meteorological evaluation of the 54.0 °C observations in Mitribah, Kuwait and Turbat, Pakistan in 2016/2017. *International Journal of Climatology*, 39, 5154–5169.
- Merlone, A., Lopardo, G., Sanna, F., Bell, S., Benyon, R., Bergerud, R.A., Bertiglia, F., Bojkovski, J., Böse, N., Brunet, M., Cappella, A., Coppa, G., del Campo, D., Dobre, M., Drnovsek, J., Ebert, V., Emardson, R., Fernicola, V., Flakiewicz, K., Gardiner, T., Garcia, C., Izquierdo, E., Georgin, A., Gilabert, A., Grykałowska, E., Grudniewicz, M., Heinonen, M., Holmsten, D., Hudoklin, J., Johansson, H., Kajastie, H., Kaykısızlı, P., Klason, L., Kňazovická, A., Lakka, A., Kowal, H., Müller, C., Musacchio, J., Nwaboh, P., Pavlasek, A., Piccato, L., Pitre, M., de Podesta, M.K., Rasmussen, H.S., Smorgon, D., Sparasci, F., Strnad, R., Szmyrka-Grzebyk, A. and Underwood, R. (2015) The MeteoMet project – metrology for meteorology: challenges and results. *Meteorological Applications*, 22, 820–829.
- Niven, D.J., Gaudet, J.E., Laupland, K.B., Mrklas, K.J., Roberts, D.J. and Stelfox, H.T. (2015) Accuracy of peripheral thermometers for estimating temperature: a systematic review and meta-analysis. *Annals of Internal Medicine*, 163, 768–777.
- Symons, G.J. (1875) On the sensitiveness of thermometers. *Quarterly Journal of the Royal Meteorological Society*, 2(11), 123–129.
- Thorne, P.W., Menne, M.J., Williams, C.N., Rennie, J.J., Lawrimore, J.H., Vose, R.S., Peterson, T.C., Durre, I., Davy, R., Esau, I.,

Klein-Tank, A.M.G. and Merlone, A. (2016) Reassessing changes in diurnal temperature range: a new data set and characterization of data biases. *Journal of Geophysical Research: Atmospheres*, **121**, 5115–5137.

World Meteorological Organization (WMO). (2014) *Guide to Meteorological Instruments and Methods of Observation (CI-MO guide)*. WMO No.8. Updated version, May 2017, p. 1139.

How to cite this article: Burt S, de Podesta M. Response times of meteorological air temperature sensors. *QJR Meteorol Soc.* 2020;146:2789–2800.
<https://doi.org/10.1002/qj.3817>